

# Low temperature luminescence of $\text{Tm}^{3+}$ ions in $\text{LiYF}_4$ crystal

Taiju Tsuboi<sup>a,\*</sup>, Hideyuki Murayama<sup>a</sup>, Kiyoshi Shimamura<sup>b</sup>

<sup>a</sup> Faculty of Engineering, Kyoto Sangyo University, Kamigamo, Kita-ku, Kyoto 603-8555, Japan

<sup>b</sup> Kagami Memorial Laboratory for Materials Science and Technology, Waseda University,  
2-8-26 Nishiwaseda, Shinjuku-ku, Tokyo 169-0051, Japan

Received 30 July 2004; received in revised form 4 December 2004; accepted 13 January 2005

Available online 13 June 2005

## Abstract

Photoluminescence and excitation spectra of  $\text{Tm}^{3+}$  ions in  $\text{LiYF}_4$  crystal have been investigated at 12 K. The ultraviolet–infrared luminescence is investigated under excitation with 780, 680, 460, 360 and 266 nm light. The different emission spectra are observed, depending on the excitation wavelength, e.g. two emission bands at 1229 and 1201 nm are generated by the 460 nm excitation but not by 780 and 680 excitation. Comparing with the excitation spectra for the IR and visible emission, we suggest the level assignment for the observed luminescence bands including the 288 and 286 nm UV emission bands.

© 2005 Elsevier B.V. All rights reserved.

**Keywords:** Luminescence; Rare-earth ions;  $\text{Tm}^{3+}$ ;  $\text{LiYF}_4$

## 1. Introduction

$\text{Tm}^{3+}$ -doped crystals have been of interest because the infrared lasers of about 1.8  $\mu\text{m}$  wavelength are important for medical applications [1–4].  $\text{Tm}^{3+}$ -doped crystals show an additional infrared emission at about 1.47  $\mu\text{m}$ . Optical communication has been currently performed using lasers operating in 1.5  $\mu\text{m}$  C-band region where silica fibers have low loss. The wavelength region of 1.45–1.50  $\mu\text{m}$  is also a low-loss region. This wavelength region will be important in near future, as it will enable us to extend the optical communication bandwidth to S-band region [5,6]. Therefore,  $\text{Tm}^{3+}$ -doped materials are useful as optical amplification device in the future optical communications.

Additionally, the  $\text{Tm}^{3+}$ -doped crystals are of interest because they generate photoluminescence (PL) in ultraviolet, blue, green and red regions. Of various  $\text{Tm}^{3+}$ -doped crystals,  $\text{Tm}^{3+}$ -doped  $\text{LiYF}_4$  (YLF) crystals are well known for the high efficient up-converted blue and red emissions [7–9]. So far considerable amount of investigation has been made on the

PL of various  $\text{Tm}^{3+}$ -doped materials including single crystals and glasses. However, few studies have been undertaken on the dependence of PL spectra on the excitation wavelength. For example, it is not clear whether the same 650–670 nm emission spectrum is generated by the excitations with light of 460, 360 and 266 nm wavelengths, which correspond to the excitation into the  $^1\text{G}_4$ ,  $^1\text{D}_2$  and  $^3\text{P}_2$  states of  $\text{Tm}^{3+}$ , respectively.

$\text{Tm}^{3+}$  ion has the  $^3\text{F}_4$ ,  $^3\text{H}_5$ ,  $^3\text{H}_4$ ,  $^3\text{F}_3$ ,  $^3\text{F}_2$ ,  $^1\text{G}_4$ ,  $^1\text{D}_2$ ,  $^1\text{I}_6$ ,  $^3\text{P}_0$ ,  $^3\text{P}_1$  and  $^3\text{P}_2$  excited states [9–12]. Of them, the possible emitting states are the  $^3\text{F}_4$ ,  $^3\text{H}_4$ ,  $^1\text{G}_4$ ,  $^1\text{D}_2$  and  $^1\text{I}_6$  states because each of these states (e.g.  $^3\text{H}_4$ ) has a relatively large energy gap for its nearby low-energy state ( $^3\text{H}_5$ ). Fluoride crystals have lower phonon energy than oxide crystals. The highest phonon energy is 556  $\text{cm}^{-1}$  in YLF [13]. Therefore, all the emitting states are expected to give rise to emission because, e.g. the gap between the  $^1\text{I}_6$  state and its nearby low-energy  $^1\text{D}_2$  states is so wide (about 7000  $\text{cm}^{-1}$ ) that the non-radiative multi-phonon relaxation is impossible in the transition from the  $^1\text{I}_6$  state to the  $^1\text{D}_2$  state. Additionally fluorides are more transparent (up to UV region) than oxides. Thus, one can expect to observe the UV emission bands due to the transitions from the  $^1\text{D}_2$  and  $^1\text{I}_6$  states. The detailed

\* Corresponding author. Tel.: +81 75 705 1899; fax: +81 75 705 1899.  
E-mail address: tsuboi@cc.kyoto-su.ac.jp (T. Tsuboi).

study, however, has not been undertaken on the luminescence due to the transitions from the high-energy  $^1I_6$  state even in YLF. In the present paper, we study the high-energy luminescence, together with the dependence of PL on the excitation wavelength.

## 2. Experimental procedure

Single crystal of 6%  $Tm^{3+}$ -doped  $LiYF_4$  (called TmYLF, hereafter) was grown in an rf-heating Czochralski furnace. The  $Tm^{3+}$  concentration is  $8.4 \times 10^{20} \text{ cm}^{-3}$ . High purity commercial yttrium fluoride, lithium fluoride and thulium fluoride were used as starting materials in the crystal growth. These compounds were melted in an iridium crucible in the Czochralski furnace under atmosphere of  $CF_4$ . The composition ratio of  $LiF$  to  $YF_3$  was 0.52:0.48. Crystal was grown at a pulling rate of 1 mm/h and rotation rate of 15 rpm. After growth the crystal was cooled down to room temperature at a rate of  $30^\circ\text{C/h}$ .

The emission and excitation spectra were measured with a Spex Fluorolog-3 fluorophotometer in 350–1600 nm spectral region. The excitation was undertaken by 450 W Xe-lamp. The excitation wavelength was selected to be 780, 680, 460, 360 and 260 nm. Absorption spectra of the crystal were measured with a Cary-5E spectrophotometer. The spectral resolution was set to be 0.2 nm. Emission and absorption spectra were measured at various temperatures between 12 K. Crystal was cooled to 12 K using a Iwatani Cryo-Mini closed-helium-gas cryostat.

## 3. Experimental results and discussion

$Tm^{3+}$  ions in YLF have absorption bands at about 1600–1780, 1120–1230, 770–800, 680–700, 645–670, 450–480, 350–365, 285–290, 280–284, 270–275 and 255–264 nm, which are due to the  $4f^{12} \rightarrow 4f^{11}5d$  electronic transitions from the  $^3H_6$  ground state to the  $^3F_4$ ,  $^3H_5$ ,  $^3H_4$ ,  $^3F_3$ ,  $^3F_2$ ,  $^1G_4$ ,  $^1D_2$ ,  $^1I_6$ ,  $^3P_0$ ,  $^3P_1$  and  $^3P_2$  states of  $Tm^{3+}$ , respectively [9–12,14]. The YLF is transparent even at 200 nm, resulting in appearance of UV  $Tm^{3+}$  absorption bands associated with high energy levels such as the  $^3P_2$  state. Various emission bands are observed at the IR to UV regions by the excitation into these states. In the following, we show various emission spectra in the IR to UV region.

Fig. 1 shows the infrared emission spectra, at 12 K, of TmYLF excited by 780, 680, 460, 360 and 260 nm light. All of these excitations give rise to the same emission bands with peaks at 1510 and 1462 nm. On the other hand, two emission bands at 1229 and 1201 nm are observed by only the 460 nm excitation. The 1229 and 1201 nm emission bands are not generated by the 780 and 680 nm excitations. They are also generated by the 360 and 260 nm excitations, but the intensities are much weaker than those generated by the 460 nm excitation. The 1510 and 1462 nm emission bands are

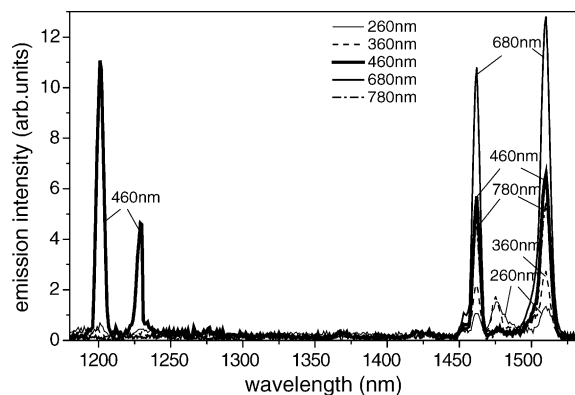


Fig. 1. Infrared emission spectra at 12 K, of  $Tm^{3+}$ -doped  $LiYF_4$  crystal excited by 780, 680, 460, 360 and 260 nm light.

attributed to the  $^3H_4 \rightarrow ^3F_4$  transition from the energy level diagram of  $Tm^{3+}$  as shown in Fig. 2.

The 1229 and 1201 nm emission bands are observed by the 460, 360 and 260 nm excitation but not by the 780 and 680 nm excitation. Therefore these emission bands are attributed to the  $^1G_4 \rightarrow ^3H_4$  transition because the  $^1G_4$  state is directly excited by the 460 nm light. The 360 and 260 nm light irradiation gives rise to the excitation into the  $^1D_2$  and  $^3P_2$  states directly, respectively, which locate at higher energy than the  $^1G_4$  state. The reason why the 360 and 260 nm excitation does not give rise to intense emission is suggested as follows. After the excitation into the  $^1D_2$  and  $^3P_2$  states, the  $Tm^{3+}$  ions are relaxed to the  $^1G_4$  state from which the ions are relaxed to the lower states radiatively and non-radiatively. It is suggested from the experimental result that, unlike the case of direct excitation into the  $^1G_4$  state, the branching ratio of the  $^1G_4 \rightarrow ^3H_4$  radiative transition is much smaller than the other ratios.

Figs. 3 and 4 show the emission spectra at 780–830 and 650–760 nm at 12 K, respectively. Quite different emission spectra are observed depending on the excitation wavelength. Emission bands at 797, 817 and 822 nm are generated by the 260, 360, 460 and 680 nm excitations, emission band at 791 nm by the 260, 360 and 460 nm excitations, while

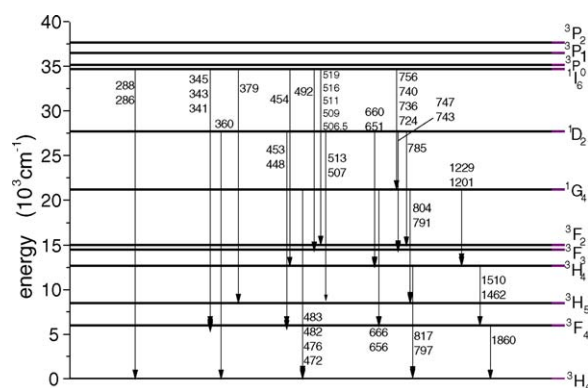


Fig. 2. Energy level diagram of  $Tm^{3+}$  and assignment of the observed  $Tm^{3+}$  emission bands in  $LiYF_4$  crystal at 12 K.

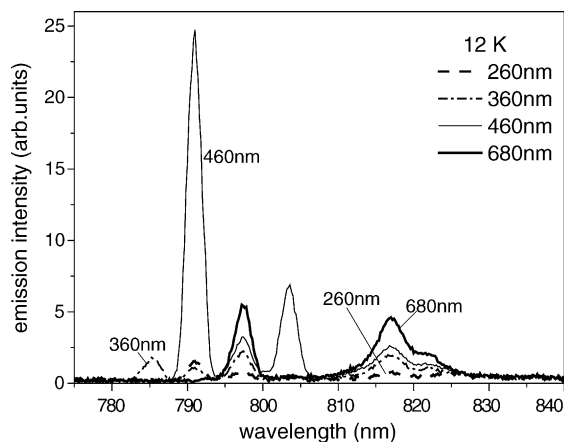


Fig. 3. Emission spectra of  $\text{Tm}^{3+}$ -doped  $\text{LiYF}_4$  excited by 880, 460, 360 and 260 nm light at 12 K.

emission band at 785 nm by only the 360 nm excitation, and emission band at 804 nm by only the 460 nm excitation. Therefore, we can attribute the 797, 817 and 822 nm bands to the  $^3\text{H}_4 \rightarrow ^3\text{H}_6$  transition, the 791 and 804 nm bands to the  $^1\text{G}_4 \rightarrow ^3\text{H}_5$  transition, and the 785 nm band to the  $^1\text{D}_2 \rightarrow ^3\text{F}_2$  transition (Fig. 2).

As seen in Fig. 4, no emission band is observed in the 700–760 nm region by the 680 and 460 nm excitations. The 460 nm excitation gives rise to emission bands at 666 and 656.5 nm, the 360 nm excitation to emission bands at 747, 743, 660, 656.5 and 651 nm, while the 260 nm excitation to emission bands at 756.5, 740, 736, 724, 666, 660 and 656.5 nm. Therefore, we can attribute the 756.5, 740, 736 and 724 nm bands to the transitions from the  $^1\text{I}_6 \rightarrow ^1\text{G}_4$  transition, the 747 and 743 nm bands to the  $^1\text{D}_2 \rightarrow ^3\text{F}_3$  transition, the 666 and 656 nm bands to the  $^1\text{G}_4 \rightarrow ^3\text{F}_4$  transition, and the 660 and 651 nm bands to the  $^1\text{D}_2 \rightarrow ^3\text{H}_4$  transition as shown in Fig. 2.

Figs. 5 and 6 show the emission spectra at 470–525 and 292–460 nm at 12 K, respectively. The 460 nm excitation gives rise to emission bands at 490, 483.5, 481.5, 476 and

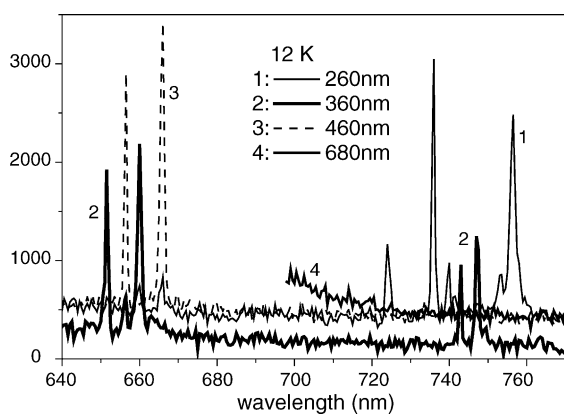


Fig. 4. Emission spectra of  $\text{Tm}^{3+}$ -doped  $\text{LiYF}_4$  crystal excited by 680, 460, 360 and 260 nm light at 12 K.

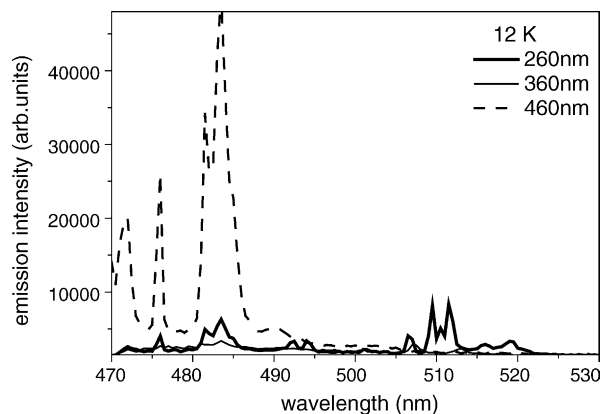


Fig. 5. Emission spectra of  $\text{Tm}^{3+}$ -doped  $\text{LiYF}_4$  crystal excited by 460, 360 and 260 nm light at 12 K.

472 nm, the 360 nm excitation to bands at 513, 507, 453 and 448.5 nm, and the 260 nm excitation to bands at 519, 516, 511.5, 509.5, 506.5, 483.5, 481.5, 476, 454.5, 450.5, 379, 360, 349.5, 345.5, 343, 341, 288 and 286 nm. The assignment for these emission bands is possible from the energy level diagram of  $\text{Tm}^{3+}$  by the same method mentioned above, which is shown in Fig. 2.

The emission spectra at room temperature are quite different from the emission spectra at 12 K. The number of the observed bands is much more at room temperature than at 12 K. This makes difficult to assign the observed bands. For example, at least 10 broad bands have been observed in the 1380–1520 nm region at room temperature [14], while only two sharp emission bands are observed in the same spectral region at 12 K as shown in Fig. 1. Several bands of such multi-bands are due to the transition from the thermally excited Stark-splitting substates of the  $^3\text{H}_4$  state [15]. The emission spectra at low temperature like 12 K exhibit the transition from the lowest substate of many Stark-splitting substates in the excited state such as  $^3\text{H}_4$ . Therefore, the observation at low temperature is useful for the level assignment for the emission bands, i.e. we obtain more reliable assignment from

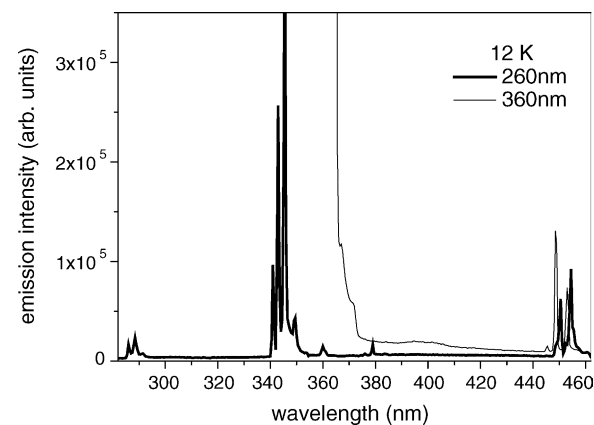


Fig. 6. Emission spectra of  $\text{Tm}^{3+}$ -doped  $\text{LiYF}_4$  crystal excited by 360 and 260 nm light at 12 K.

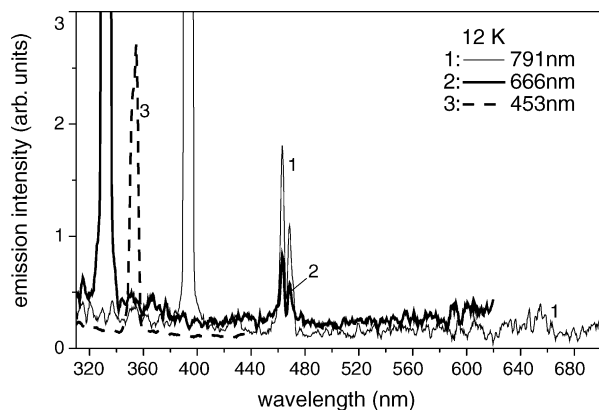


Fig. 7. Excitation spectra for 791, 666 and 453 nm emissions of  $\text{Tm}^{3+}$ -doped  $\text{LiYF}_4$  crystal at 12 K.

the low-temperature luminescence than from the luminescence at room temperature.

Fig. 7 shows the excitation spectra for the 791, 666 and 453 nm emission at 12 K. Two intense bands at about 395 and 333 nm are due to the half harmonic of the 791 and 666 nm emission, respectively. The 791 nm emission is generated by the excitation of the 460–470 nm absorption bands (due to the  $^3\text{H}_6 \rightarrow ^1\text{G}_4$  transition), but it is not generated by the excitation of the 355–360 nm absorption bands (due to the  $^3\text{H}_6 \rightarrow ^1\text{D}_2$  transition). Unlike the 797 and 817 nm emission bands, the 791 nm emission is not generated by the excitation of the 660–700 nm absorption bands (due to the  $^3\text{H}_6 \rightarrow ^3\text{F}_2$  and  $^3\text{F}_3$  transitions). This indicates that neither the multiphonon non-radiative process nor radiative transition occurs in the relaxation from the  $^1\text{D}_2$  excited state into the nearby lower-energy state  $^1\text{G}_4$ .

Regarding the 666 nm emission, it is generated by the excitation of the 460–470 nm absorption bands (due to the  $^3\text{H}_6 \rightarrow ^1\text{G}_4$  transition). Unlike the 660 and 651 nm emission bands, it is not generated by the excitation of the 355–360 nm absorption bands (due to the  $^3\text{H}_6 \rightarrow ^1\text{D}_2$  transition). This shows that the different electronic transition is responsible between the 666 and 660 nm emission bands although these emission wavelengths are close to each other. Therefore, our level assignment for the 666 and 660 nm emission bands (shown in Fig. 2) is confirmed by the excitation spectra and the absence of both non-radiative and radiative transitions from the  $^1\text{D}_2$  state to the  $^1\text{G}_4$  state, because, if one of such transitions occur, the 666 nm emission should be generated by the excitation into the  $^1\text{D}_2$  state with 355–360 nm light.

Regarding the 453 nm emission, it is generated by the excitation into the 355–360 nm band (due to the  $^3\text{H}_6 \rightarrow ^1\text{D}_2$  transition). We assigned this emission to the  $^1\text{D}_2 \rightarrow ^3\text{F}_4$  transition from the emission spectrum measurement (Fig. 2). This is consistent with the result of excitation spectrum. In this

way, we can confirm the optical process shown in Fig. 2 by the excitation spectra.

#### 4. Summary

Photoluminescence and excitation spectra of  $\text{Tm}^{3+}$  ions in  $\text{LiYF}_4$  crystal have been investigated at 12 K. The luminescence that appeared in infrared, visible and ultraviolet regions is investigated under excitation with 780, 680, 460, 360 and 266 nm light. The PL spectra are quite different from the spectra at room temperature. For example, unlike the case of 290 K with at least ten broad emission bands, only two sharp emission bands are observed at 1510 and 1462 nm in the 1400–1550 nm region. The 1510 and 1462 nm bands are generated by the excitation with 780, 680, 460, 360 and 266 nm. It is observed, however, that two emission bands at 1229 and 1201 nm are generated by the 460 nm excitation but not by 780 and 680 nm excitation. Such a dependence of emission bands on the excitation wavelength is observed in various emission bands from near-IR to UV region. Comparing with the results of excitation spectra, we suggest the level assignment for all the observed luminescence bands. For example, the 666 and 656 nm bands are attributed to the  $^1\text{G}_4 \rightarrow ^3\text{F}_4$  transition, while the 660 and 651 nm bands, which locate close to the 666 and 656 nm bands, to the  $^1\text{D}_2 \rightarrow ^3\text{H}_4$  transition.

#### References

- [1] G.L. Bourdet, G. Lescroart, R. Muller, *Opt. Commun.* 150 (1998) 141.
- [2] F. Cornacchia, A. Di Lieto, P. Maroni, P. Minguzzi, A. Toncelli, M. Tonelli, E. Sorokin, I.T. Sorokina, *Appl. Phys. B* 73 (2001) 191.
- [3] V. Sudesh, K. Asai, K. Shimamura, T. Fukuda, *IEEE J. Quantum Electron.* 38 (2002) 1102.
- [4] V. Sudesh, K. Asai, *J. Opt. Soc. Am. B* 20 (2003) 1829.
- [5] T. Komukai, T. Yamamoto, T. Sugawa, Y. Miyajima, *IEEE J. Quantum Electron.* 31 (1995) 1880.
- [6] S. Kawanishi, K. Uchiyama, H. Takara, T. Morioka, M. Yamada, T. Kanamori, *Electron. Lett.* 33 (1997) 1553.
- [7] G. Özen, B. Di Bartolo, *Appl. Phys. B* 70 (2000) 189.
- [8] G. Özen, S. Salihoglu, *Opt. Commun.* 180 (2000) 323.
- [9] A. Brener, J. Rubin, R. Moncorge, C. Pedrini, *J. Phys.* 50 (1989) 1463.
- [10] T. Tsuboi, Y.F. Ruan, N. Kulagin, in: J.C. Krupa, N.A. Kulagin (Eds.), *Physics of Laser Crystals, NATO SCIENCE SERIES: II. Mathematics, Physics and Chemistry*, vol. 126, Kluwer Science Publishers, London, 2003, pp. 171–185 (Chapter 12).
- [11] T. Tsuboi, M. Tanigawa, K. Shimamura, *Opt. Commun.* 186 (2000) 127.
- [12] T. Tsuboi, *J. Electrochem. Soc.* 147 (2000) 1997.
- [13] J. Sytsma, G.F. Imbusch, G. Blasse, *J. Phys.: Condens. Matter* 2 (1990) 5171.
- [14] T. Tsuboi, K. Shimamura, *SPIE Proc.* 5460 (2004) 187.
- [15] T. Tsuboi, K. Shimamura, *Rare Earths* 44 (2004) 120 (in Japanese).